

Protective Role of Aquaporin-4 Water Channels after Contusion Spinal Cord Injury

Atsushi Kimura, MD, PhD,^{1,2,3} Mike Hsu, MS,^{1,2,4} Marcus Seldin, BS,^{1,2}
 Alan S. Verkman, MD, PhD,^{5,6} Helen E. Scharfman, PhD,⁷
 and Devin K. Binder, MD, PhD^{1,2,4}

Objective: Spinal cord injury (SCI) is accompanied by disruption of the blood-spinal cord barrier and subsequent extravasation of fluid and proteins, which results in edema (increased water content) at the site of injury. However, the mechanisms that control edema and the extent to which edema impacts outcome after SCI are not well elucidated.

Methods: Here, we examined the role of aquaporin-4 (AQP4) water channels after experimental contusion injury in mice, a clinically relevant animal model of SCI.

Results: Mice lacking AQP4 (AQP4^{-/-} mice) exhibited significantly impaired locomotor function and prolonged bladder dysfunction compared with wild-type (WT) littermates after contusion SCI. Consistent with a greater extent of functional deterioration, AQP4^{-/-} mice showed greater neuronal loss and demyelination, with prominent cyst formation, which is generally absent in mouse SCI. The extent of spinal cord edema, as expressed by percentage water content, was persistently increased above control levels in AQP4^{-/-} mice but not WT mice at 14 and 28 days after injury. Immunohistochemical analysis indicated that blood vessels in the vicinity of the lesion core had incomplete barrier function because of sparse tight junctions.

Interpretation: These results suggest that AQP4 plays a protective role after contusion SCI by facilitating the clearance of excess water, and that targeting edema after SCI may be a novel therapeutic strategy.

ANN NEUROL 2010;67:794–801

Spinal cord injury (SCI) is accompanied by disruption of the blood-spinal cord barrier and subsequent extravasation of fluid and proteins, which results in edema at the site of injury.¹ Edema at the injury site appears to develop in close association with necrosis at the lesion epicenter, and spreads bidirectionally along the cord within 24 to 48 hours after trauma.² A greater extent of spinal cord edema, evaluated by magnetic resonance imaging, has been correlated with worse neurological outcome.^{3–5} Edema is thought to be exacerbated by release of cytokines and proteases from activated astrocytes, microglia, and leukocytes.⁶ However, the mechanisms that control edema and the extent to which edema impacts outcome after SCI are not known. A better understanding of these

mechanisms may lead to novel strategies to attenuate secondary injury.

Aquaporin-4 (AQP4) is a molecular water channel in the brain and spinal cord that is predominantly expressed in astrocytic processes (end-feet) in direct contact with blood vessels.⁷ The expression of AQP4 in the spinal cord is prominent not only in astrocytic end-feet but also at the glia limitans, where the spinal cord directly contacts cerebrospinal fluid.⁸ This pattern of expression suggests that AQP4 may play a crucial role in spinal cord water homeostasis. It has recently been demonstrated that AQP4 is upregulated at the site of injury where astroglia proliferate (“astroglial scarring”) after SCI.^{9,10} Therefore, AQP4 could contribute to the outcome after SCI, and in

Published online in Wiley InterScience (www.interscience.wiley.com). DOI: 10.1002/ana.22023

Received Aug 17, 2009, and in revised form Feb 12, 2010. Accepted for publication Mar 5, 2010.

Address correspondence to Dr Binder, Center for Glial-Neuronal Interactions, Division of Biomedical Sciences, University of California, Riverside, 900 University Ave., Riverside, CA 92521-0121. E-mail: dbinder@ucr.edu

From the ¹Department of Neurological Surgery and ²Department of Anatomy and Neurobiology, University of California, Irvine, CA; ³Department of Orthopedics, Jichi Medical University, Tochigi, Japan; ⁴Center for Glial-Neuronal Interactions, Division of Biomedical Sciences, University of California, Riverside, CA; ⁵Department of Medicine and ⁶Department of Physiology, University of California, San Francisco, CA; and ⁷Nathan Kline Institute for Psychiatric Research, Orangeburg, NY.

Additional Supporting Information can be found in the online version of this article.

a model of compression injury, evidence for this hypothesis was provided.¹¹ Here, we examined the role of AQP4 after contusion SCI, a clinically relevant type of SCI.^{12,13} We demonstrate that contusion SCI in AQP4^{-/-} mice leads to significantly worse outcome relative to control mice. Interestingly, this result would not have been predicted by the earlier studies of AQP4^{-/-} mice after compression SCI.¹¹ Taken together, the results suggest that the role of AQP4 is dependent on the type of SCI, which has implications for treatment of SCI.

Materials and Methods

Animals

Adult female wild-type (WT) and AQP4^{-/-} mice were bred on a CD1 background as described.¹⁴ Animals were housed under controlled conditions (12-hour day-night cycle) and were allowed access to food and water ad libitum. All procedures were carried out with the approval of the University of California-Irvine Institutional Animal Care and Use Committee.

Contusion SCI

Animals were anesthetized with ketamine/xylazine, and a laminectomy was performed at the T10 vertebral level. Contusion SCI was induced by the Infinite Horizons impactor (Infinite Horizons, Lexington, KY) using a force of 60 kdyn. Postoperative care consisted of buprenorphine (0.05mg/kg subcutaneously [sc]) twice daily for 2 days, lactated Ringer's (50ml/kg sc) once daily for 5 days, and Baytril (2.5µg/kg, sc) once daily for 2 weeks.

Locomotor Function

The recovery of open-field locomotor performance was evaluated using the Basso Mouse Scale (BMS).^{15,16} Mice were observed individually for 4 minutes each in an open field by 2 investigators blinded to genotype. Hindlimb motor function was recorded and scored according to the BMS guidelines once per week. All open-field BMS score episodes were recorded using a videocamera and reviewed later to confirm accuracy.

Footprint Analysis

Footprint analysis was conducted to assess stepping patterns of forelimbs and hindlimbs at 42 days postinjury (DPI). Animals were required to run along a paper-lined runway to obtain an edible treat in a darkened box. The plantar surfaces of forelimbs and hindlimbs were brushed with red and black nontoxic paint, respectively. Quantitative analysis was performed on stride length, toe drags, and footprint width.¹⁷ One toe drag was counted when the ink streak from a hind paw was longer than 1 paw length and located between 2 hindlimb footprints on the same side. Footprint width was defined as the distance between the heel spots of the 2 hindlimbs. Each session consisted of 3 separate traverses of the track. Footprints were scanned, and digitized images were measured. For analyses, at least 5 steps from each side from 3 sessions were measured per animal per group.

Residual Urine

After SCI there is a loss of bladder control, and the bladder must be emptied regularly by manual expression (method of Crede) to prevent urinary tract infection. Manual bladder expression was performed twice daily until sufficient recovery of bladder function. Residual urine weight was recorded at 1, 3, 7, 21, 28, 35, and 42 DPI.

Bladder Weight and Volume

The bladder was removed at 42 DPI, emptied of urine, blotted dry, and weighed. Total bladder volume was calculated based on the size of the bladder, as described previously.¹⁸ Briefly, the perpendicular length (L) and width (W) were measured, and the formula for a prolate spheroid ($\frac{4}{3} \times \pi \times L \times [W/2]^2$) was used to estimate total bladder volume.

Tissue Processing

At designated time points after injury, mice were deeply anesthetized with sodium pentobarbital and perfused intracardially with phosphate-buffered saline (PBS) and 4% paraformaldehyde. Spinal cords were removed and postfixed for 2 hours before they were rinsed and immersed in PBS overnight. The following day, tissues were immersed in 30% sucrose for 48 hours, then were blocked into 5-mm segments centered on the injury site before embedding in OCT. Ten-micrometer cross or 20-µm longitudinal frozen sections were serially sectioned and collected.

Immunohistochemical Analysis

Sections were permeabilized with 0.3% Triton X-100, blocked with 5% normal horse serum in 0.1 M PBS, then incubated with primary antibody to neuronal-specific nuclear protein (NeuN; 1:200; Millipore, Temecula, CA) and fibronectin (1:200; Sigma, St Louis, MO) at 4°C overnight. After rinsing with PBS, sections were incubated with a species-specific secondary antibody conjugated with Alexa 488, 594, or 647 (Molecular Probes/Invitrogen, Carlsbad, CA) for 1 hour at room temperature, and then mounted in Vectorshield containing 4',6-diamidino-2-phenylindole (Vector Laboratories, Burlingame, CA). Images were obtained by fluorescence microscopy (BX51; Olympus, San Diego, CA) or confocal microscopy (LSM510; Carl Zeiss, Thornwood, NY).

Terminal Deoxynucleotidyl Transferase dUTP Nick-End Labeling Staining

Three consecutive sections centered at 1mm rostral and caudal to the injury epicenter were processed for terminal deoxynucleotidyl transferase dUTP nick-end labeling (TUNEL) staining (ApopTag Fluorescein In Situ Apoptosis Detection Kit, Millipore). Mean numbers of TUNEL-positive cells at each point were calculated for each genotype at 7 and 42 DPI.

Lesion Size and Spared White Matter

For quantification of lesion size, serial sections of the spinal cord at 42 DPI were used. For quantification of spared white matter, Luxol fast blue (LFB) staining was performed, and areas of spared white matter were calculated by the Cavalieri method. A point grid was made using Adobe Illustrator and superimposed

onto images of the cross sections at 250 μ m intervals, centered at the lesion epicenter. The epicenter was defined as the section containing the least amount of spared white matter. Points included in the spared white matter were counted by Scion Image (Scion Corporation, Frederick, MD), and point tallies were converted into area estimates using the formula $area = a/p \times \Sigma P$, where a/p equals the area represented by each point, and ΣP equals the number of points counted in each image. Percent spared white matter area was calculated by dividing the measured areas of spared myelin by the average white matter area at the T10 level of sham-operated controls.

For quantification of lesion volume, serial cross sections were immunostained for fibronectin to delineate the lesion border. When cysts were found within the lesion, cyst area was counted as part of the lesion. Twelve sections at 250 μ m intervals rostral and caudal to the lesion epicenter were used for this analysis. Lesion areas calculated by the Cavalieri method were converted into volume estimates using the formula $volume = T \times a/p \times \Sigma P$, where T is the distance between sections.

NeuN-positive cells were counted using tissue from mice that were perfused at 7 and 42 DPI. Serial cross sections were immunostained for NeuN, and digital images were captured. The section that had the lowest number of NeuN-positive cells was designated as the lesion epicenter, and 4 rostral and 4 caudal sections at intervals of 500 μ m were analyzed. All of the NeuN-positive cells in each cross section were counted manually by investigators blinded to genotype. Sham controls (T10 laminectomy) were analyzed in the same manner.

Spinal Cord Edema Measurement

Water content of the spinal cord was measured by a wet-dry method to provide a quantitative measure of edema. At each time point, animals with SCI were deeply anesthetized with pentobarbital. Five-millimeter lengths of spinal cords centered at the injury epicenter were immediately removed and weighed, then dried at 85°C for 48 hours, and reweighed. Percent water content was calculated as $(wet\ weight - dry\ weight) / wet\ weight \times 100$.

Statistics

Using SPSS (SPSS Inc., Chicago, Ill), data for the BMS, BMS subscores, and residual urine weight were analyzed by repeated-measures analysis of variance (ANOVA) with post hoc Bonferroni test. Histological assessments for number of NeuN⁺ cells and percentage spared myelin were analyzed using a 2-way ANOVA with post hoc Bonferroni test. The unpaired t test or Mann-Whitney U test was also used for other analyses as indicated in the figure legends. Differences were considered significant at $p < 0.05$.

Results

Impaired Locomotor Recovery in AQP4^{-/-} Mice after Contusion SCI

To evaluate the effects of AQP4 deficiency on locomotor recovery after SCI, we assessed locomotor function using the 9-point BMS scale, which is widely used to evaluate hindlimb motor function in mice in an open field.¹⁵ SCI

caused severe disabilities in both genotypes, as assessed by the BMS score at 1 DPI of 0.05 and 0, respectively, indicative of almost no ankle joint movement. Although both groups subsequently exhibited gradual recovery in hindlimb function, AQP4^{-/-} mice had significantly worse BMS scores than WT mice ($p = 0.0155$). BMS scores differed significantly at 7, 14, 28, 35, and 42 DPI (Fig 1A). BMS subscores, which quantify improvements in stepping frequency, coordination, paw position, trunk stability, and tail position, was also much lower in AQP4^{-/-} mice compared to WT mice ($p = 0.0045$, repeated-measures ANOVA) and was significantly different at 14, 28, 35, and 42 DPI (see Fig 1B).

In addition, we analyzed the plantar stepping patterns of forelimbs and hindlimbs using footprint analysis at 42 DPI. Footprints from AQP4^{-/-} mice showed significantly decreased stride length, width of hindlimb footprints, and increased toe dragging (see Fig 1C–G). Taken together, these data indicate that the absence of AQP4 is associated with significantly worse motor recovery after SCI.

Prolonged Bladder Dysfunction in AQP4^{-/-} Mice after SCI

To assess the effect of AQP4 deficiency on recovery of autonomic function, we examined changes in residual urine after SCI. Before injury, manual expression of the bladder demonstrated that mice retain no or minimal urine. In contrast, SCI caused severe urinary retention in both WT and AQP4^{-/-} mice. After SCI, residual urine weight peaked at 3 DPI, and WT mice exhibited a gradual recovery in urinary retention on subsequent days, but there was prolonged bladder dysfunction in AQP4^{-/-} mice throughout the 42-day observation period (see Fig 2A). Residual urine weight was significantly greater in AQP4^{-/-} mice compared to WT mice ($p = 0.0019$); post hoc tests revealed that residual urine differed significantly at 28, 35, and 42 DPI.

We also measured bladder weight and volume at 42 DPI. Bladder weight (wet weight after eliminating urine) of AQP4^{-/-} mice was significantly heavier than that of WT mice ($p = 0.0327$) (see Fig 2B). The estimated bladder volume, based on the calculated bladder size, was also significantly larger in AQP4^{-/-} mice than WT mice ($p = 0.0024$) (see Fig 2C). These significant changes in bladder morphology confirmed that there was sustained bladder dysfunction in AQP4^{-/-} mice during the observation period.

Greater Demyelination, Lesion Volume, Cyst Formation, and Neuronal Loss in AQP4^{-/-} Mice

To assess the histological basis of the functional deficits in AQP4^{-/-} mice after SCI, we examined myelin sparing

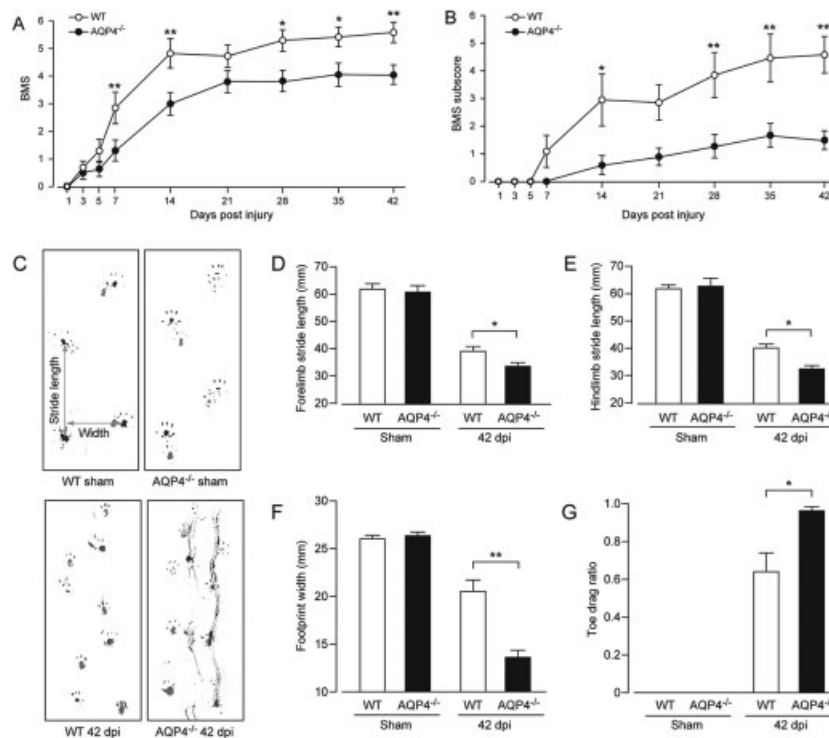


FIGURE 1: Impaired locomotor recovery after contusion spinal cord injury in aquaporin-4 (AQP4)^{-/-} mice. AQP4^{-/-} mice had worse functional outcome as revealed by Basso Mouse Scale (BMS) (A) and BMS subscores (B) compared with wild-type (WT) mice (white circles, WT; black circles, AQP4^{-/-}). Data are represented as mean \pm standard error of the mean (SEM), $n = 10$ for each group. Statistical comparisons were made using repeated-measures analysis of variance with Bonferroni post hoc test, $*p < 0.05$, $**p < 0.01$. (C) Representative images of footprint analysis (upper left, WT sham; lower left, WT 42 days postinjury [DPI]; upper right, AQP4^{-/-} sham; lower right, AQP4^{-/-} 42 DPI). AQP4^{-/-} mice showed significantly decreased stride length in both forelimbs (D) and hindlimbs (E), decreased width of hindlimb footprints (F), and increased toe drag ratio (G) (white bars, WT; black bars, AQP4^{-/-}). Data are represented as mean \pm SEM, $n = 10$ for each group. Statistical significance was evaluated using a Student t test or Mann-Whitney U test, $*p < 0.05$, $**p < 0.01$.

using LFB staining at 42 DPI. Spared myelin was significantly reduced in AQP4^{-/-} mice compared to WT mice ($p = 0.0323$, repeated-measures ANOVA; Fig 3). AQP4^{-/-} mice also showed consistent cyst formation, which is usually absent or small after SCI in mice.^{19,20} Cyst volume was significantly larger in AQP4^{-/-} mice compared to WT mice. Lesion volume was also significantly larger in AQP4^{-/-} mice compared to AQP4 WT mice ($p = 0.0012$).

We assessed the number of NeuN-positive cells at 42 DPI in 4mm-long segments centered at the injury epicenter. This revealed a significantly reduced NeuN-positive cell number in AQP4^{-/-} mice ($p = 0.0134$, repeated-measures ANOVA; Fig 4A and B), and analysis of specific spinal segments revealed significant differences between AQP4^{-/-} mice and WT mice at 1,500 μ m cranial, 500 μ m caudal, 1,000 μ m caudal, and 1,500 μ m caudal to the lesion epicenter (Bonferroni post hoc tests; see Fig 4B). These results suggest that AQP4 deficiency increases lesion volume and neuronal loss after SCI. This neuronal loss may be slow and progressive, because less neuronal loss was observed at 7 days DPI in a separate

analysis (Supplemental Fig 1). As an indicator of apoptotic cells, we performed TUNEL staining at 7 and 42 DPI. Cells positive for TUNEL were counted at sections 1mm rostral and caudal to the injury epicenter. At 7 DPI, AQP4^{-/-} mice had a significantly greater number of TUNEL⁺ cells compared to WT mice both rostral and caudal to the injury epicenter (see Fig 4C and D). The difference between genotypes remained significant in sections 1mm caudal to the epicenter at 42 DPI.

Persistent Water Accumulation at the Site of SCI in AQP4^{-/-} Mice

We examined the magnitude of edema (spinal cord water content) at the site of SCI at 2, 7, 14, and 28 DPI using the wet-dry method. Because there was a slight difference in water content of control WT versus control AQP4^{-/-} mice, we decided to compare percentage change in water content relative to controls. Spinal cord edema reached a maximum level at 2 DPI and returned to control levels by 14 DPI in WT mice (Fig 5). In contrast, in AQP4^{-/-} mice, water content of the in-

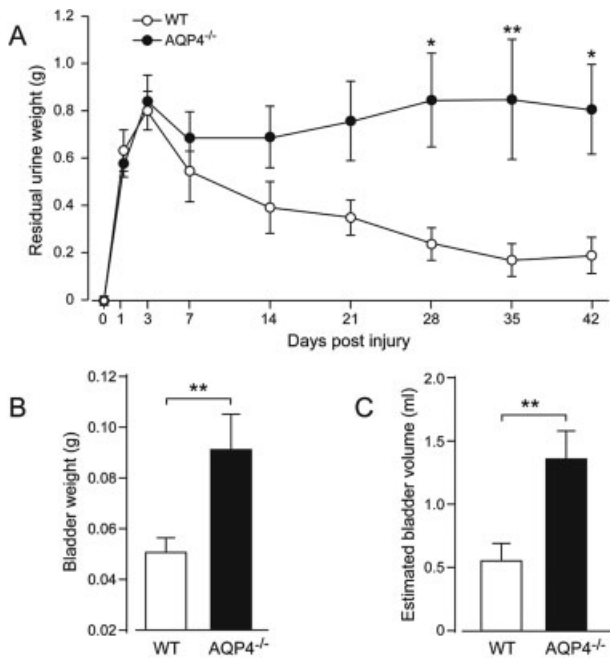


FIGURE 2: Prolonged bladder dysfunction after spinal cord injury in aquaporin-4 (AQP4)^{-/-} mice. AQP4^{-/-} mice had prolonged bladder dysfunction relative to wild-type (WT) mice; dysfunction was evaluated by residual urine (white circles, WT; black circles, AQP4^{-/-}) (A). Data are represented as mean \pm standard error of the mean (SEM), $n = 14$ for each group. Statistical comparisons were made using repeated-measures analysis of variance with Bonferroni post hoc test, * $p < 0.05$, ** $p < 0.01$. Consistent with the chronic bladder dysfunction, bladder weight (wet weight after eliminating urine) (B) and estimated bladder volume (C) were significantly higher in AQP4^{-/-} mice. Data are represented as mean \pm SEM, $n = 14$ for each group; statistical comparisons used a Student t test, ** $p < 0.01$.

jured spinal cord remained elevated above control levels at 14 and 28 DPI (see Fig 5).

Discussion

In this study, we demonstrated that compared with WT littermates, AQP4^{-/-} mice exhibit significantly impaired locomotor function, prolonged bladder dysfunction, greater tissue damage with prominent cyst formation, and increased tissue water content after contusion SCI. These results suggest that AQP4 plays a protective role after contusion SCI by facilitating the clearance of tissue water.

Bidirectional Regulation of Central Nervous System Edema by AQP4

Perivascular AQP4 allows bidirectional water flow and is suggested to be critically involved in the formation as well as clearance of edema.⁷ AQP4 deficiency improves neurological outcome in models of cytotoxic (cellular) edema such as water intoxication and ischemia,²¹ but worsens outcome in models of vasogenic (fluid leak) edema, in-

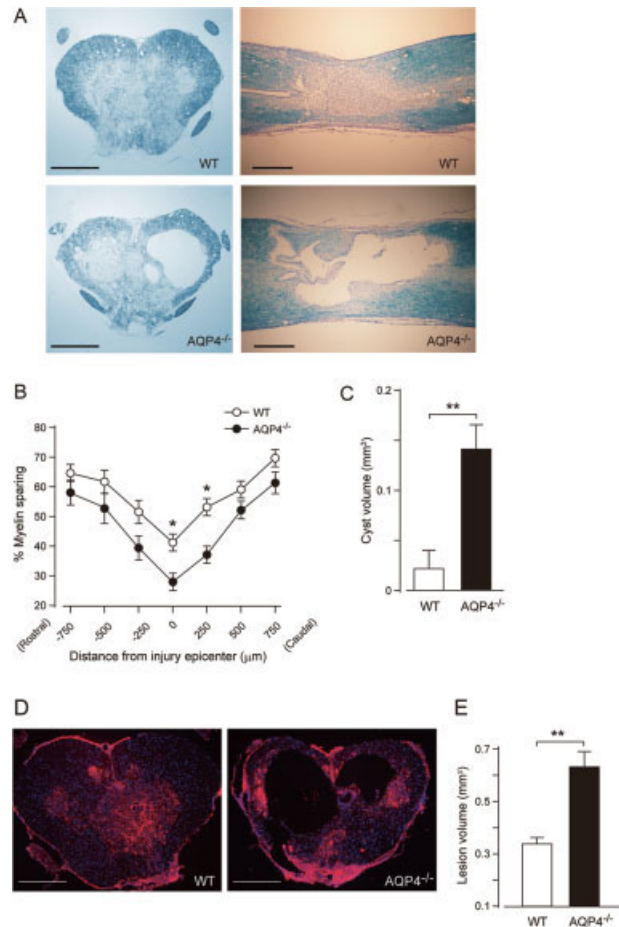


FIGURE 3: Greater tissue damage and prominent cyst formation in aquaporin-4 (AQP4)^{-/-} mice. (A) Representative images of Luxol fast blue (LFB) staining at 42 days postinjury (upper left, wild-type [WT] cross section; upper right, WT longitudinal section; lower left, AQP4^{-/-} cross section; lower right, AQP4^{-/-} longitudinal section). Note the greater demyelination and prominent cyst formation in AQP4^{-/-} mice. (B) Stereological quantification of LFB staining shows significantly increased myelin loss in AQP4^{-/-} mice. Data are represented as mean \pm standard error of the mean (SEM), $n = 7$ for each group; statistical significance was evaluated using a 2-way analysis of variance with Bonferroni post hoc test, * $p < 0.05$. (C) Quantification of cyst volume shows significantly greater cyst volume in AQP4^{-/-} mice (black bar) compared with WT mice (white bar). Data are represented as mean \pm SEM, $n = 7$ for each group; statistical comparisons were made using Student t test, ** $p < 0.01$. (D) Representative images of fibronectin staining at the injury epicenter (red, fibronectin; blue, 4',6-diamidino-2-phenylindole; left, WT; right, AQP4^{-/-}). (E) Stereological quantification of lesion volume delineated by fibronectin shows significantly greater lesion volume in AQP4^{-/-} mice (black bar) compared with WT mice (white bar). Data are represented as mean \pm SEM, $n = 7$ for each group; statistical comparisons used Student t test, ** $p < 0.01$. Scale bars = 400 μ m. [Color figure can be viewed in the online issue, which is available at www.interscience.wiley.com.]

cluding cortical freeze-injury, brain tumor, and brain abscess.^{22,23}

Contusion SCI, which can be considered a clinically relevant model of SCI, causes significant disruption of blood vessels, leading to extravasation of plasma pro-

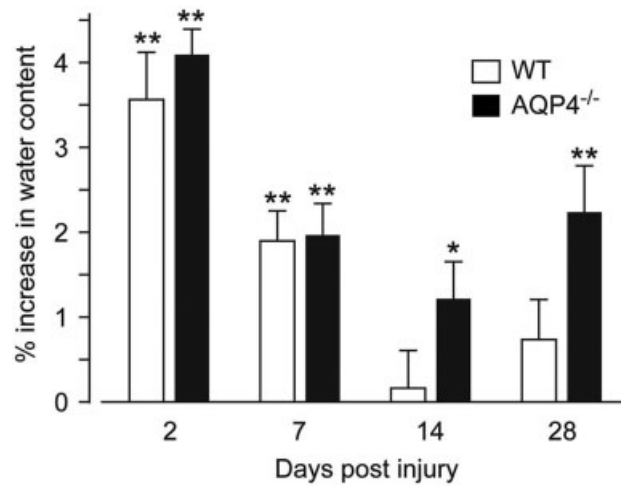
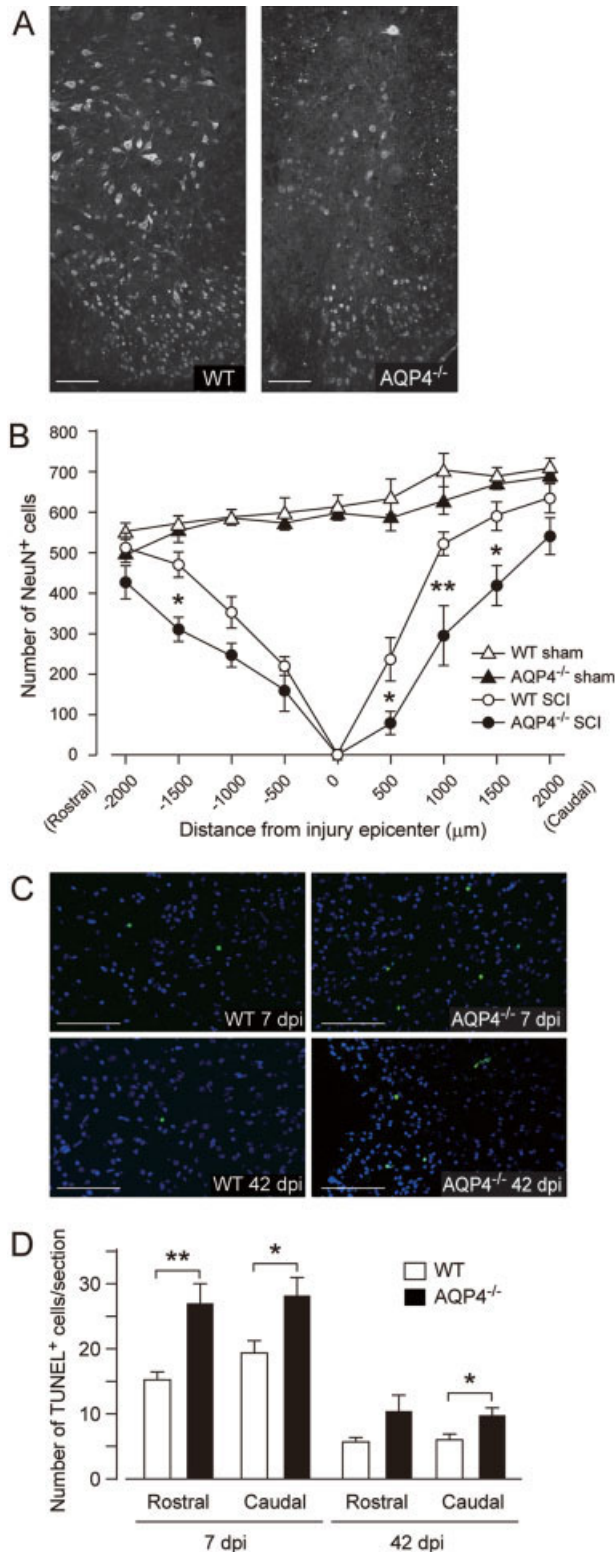


FIGURE 5: Persistent water accumulation in aquaporin-4 (AQP4)^{-/-} spinal cords. Time course of edema after spinal cord injury as expressed by change in percentage of water content [(wet - dry)/wet × 100] relative to genotype control. The increase in water content peaked at 2 days postinjury in both genotypes. In wild-type (WT) mice, spinal cord water content at days 14 and 28 was not significantly different from control. In contrast, AQP4^{-/-} mice demonstrated persistently increased spinal cord water content at 14 and 28 days. Data are represented as mean ± standard error of the mean, n = 5 to 7 for each group. Comparisons were evaluated using Student t test, *p < 0.05, **p < 0.01.

FIGURE 4: Greater neuronal loss and apoptotic cell death in aquaporin-4 (AQP4)^{-/-} mice. (A) Representative images of neuronal-specific nuclear protein (NeuN) staining at 42 days postinjury (DPI), 1mm caudal of lesion epicenter (left, wild-type [WT]; right, AQP4^{-/-}). Note the greater loss of neurons in AQP4^{-/-} mice. (B) Stereological estimation of NeuN-positive cells at 42 DPI. At 1mm caudal to the lesion epicenter, there was almost a 40% greater loss of neurons in AQP4^{-/-} mice compared to WT mice. Data are represented as mean ± standard error of the mean (SEM), n = 7 for each group (n = 3 for sham controls); statistical comparisons used a 2-way analysis of variance with Bonferroni post hoc test, *p < 0.05, **p < 0.01. (C) Representative images of terminal deoxynucleotidyl transferase dUTP nick-end labeling (TUNEL) staining after spinal cord injury (SCI) at 7 and 42 DPI (green, TUNEL; blue, 4',6-diamidino-2-phenylindole). (D) Quantification of TUNEL⁺ cells at sections 1mm rostral and caudal to the injury epicenter. Note the greater number of TUNEL⁺ cells in AQP4^{-/-} mice compared to WT mice, both rostral and caudal to the injury epicenter at 7 DPI. The difference between genotypes remained significant in sections 1mm caudal to the epicenter at 42 DPI. Data are represented as mean ± SEM, n = 5 for each group; statistical comparisons used a Student t test, *p < 0.05, **p < 0.01. Scale bars: = 100μm. [Color figure can be viewed in the online issue, which is available at www.interscience.wiley.com.]

teins.²⁴ As such, it appears to be predominantly a model of vasogenic edema. Recently, Saadoun et al demonstrated improved neurological outcome after spinal cord compression injury in AQP4^{-/-} mice.¹¹ These opposite results may be explained by mechanisms underlying the 2 different SCI models. The authors induced SCI by bilateral compression of the thoracic spinal cord for 2 minutes. The compression SCI model is thought to induce ischemia, which is a model of cytotoxic edema.^{25,26} Given the different mechanisms of injury initiated using the 2 SCI models (cytotoxic vs vasogenic), we suggest that the role of AQP4 is dependent on the type of injury. Therefore, potential therapeutic strategies that are based on AQP4 or other regulators of edema should take into account the type of injury. In experimental SCI, it may not be possible to generalize results from models that use only compression or only contusion.

AQP4 Deficiency Exacerbates Tissue Damage after Contusion SCI

Several possible mechanisms may account for increased tissue damage in AQP4^{-/-} mice after SCI. First, elimination of edema fluid is impaired in AQP4^{-/-} mice with vasogenic edema.²³ We observed an increase in water content at late time points after SCI in AQP4^{-/-} mice compared with WT mice (see Fig 5), coinciding with a progressive loss of neurons in AQP4^{-/-} mice (see Fig 4, Supplemental Fig 1). Because hypo-osmolar stress induces neuronal apoptosis through p75 neurotrophin receptor expression,²⁷ water accumulation around the lesion core could trigger hypo-osmolar stress and increased apoptosis (see Fig 4C and D). A second possible mechanism is excitotoxic cell death due to impaired clearance of glutamate through the glial glutamate transporter EAAT-2.^{28,29} Because glutamate excitotoxicity plays a key role not only in neuronal cell death but also in delayed posttraumatic white matter degeneration after SCI,³⁰ impaired glutamate clearance associated with AQP4 deficiency could lead to the increased tissue damage observed in AQP4^{-/-} mice. A third possible mechanism is impaired formation of the astroglial scar in AQP4^{-/-} mice,³¹ as rapid migration of reactive astrocytes is suggested to be essential for restricting inflammation and lesion size.^{32,33}

Prominent Cyst Formation at the Site of SCI in AQP4^{-/-} Mice

Mouse SCI models rarely exhibit the progressive necrosis and cavitation that is usually seen in rats and other mammals.^{20,34} Instead, acute necrotic cavities develop in WT mice, and become filled with fibrous connective tissue.¹⁹ In contrast, AQP4^{-/-} mice exhibit fluid-filled cystic cavities at the site of injury (see Fig 3); persistently increased

water content at the site of injury (up to 28 DPI; see Fig 5); and leaky blood vessels with immature tight junctions around the lesion core even as late as 42 DPI (Supplemental Fig 2). Therefore, AQP4 may play an important role in the elimination of tissue water in the vicinity of the lesion core. Similarly, it has been recently demonstrated that kaolin-induced hydrocephalus is accelerated in AQP4^{-/-} mice.³⁵ This finding is significant, because impaired recovery after SCI is often partially attributed to the fluid-filled cysts that form a physical barrier within the injured spinal cord.

Potential Role of AQP4 as a Therapeutic Target after SCI

Functional modulation of AQP4 has been proposed as a novel therapeutic strategy for a variety of central nervous system disorders associated with edema, because AQP4 provides the major route for water transport across glial cell membranes.⁷ Our data suggest that pharmacological induction of AQP4 expression may restrict secondary damage, cyst formation, and accompanying functional deterioration after contusion SCI. This approach might be particularly useful in specific syndromes such as post-traumatic syringomyelia, or cystic degeneration of the spinal cord, which develops in up to 30% of patients after SCI and is associated with progressive neurological impairment, including sensorimotor deficits, neuropathic pain, and autonomic dysfunction.³⁶ Therefore, given the role of AQP4 in spinal cord water homeostasis after injury, targeting edema clearance may be a novel therapeutic strategy for treatment of contusion injuries to the spinal cord.

Acknowledgments

This work was supported by a New York State Spinal Cord Injury Research Program grant (to H.E.S. and D.K.B.) and a grant from the Nakatomi Foundation (to A.K.).

We thank K. Sharp for assistance with spinal cord injury.

Potential Conflicts of Interest

Nothing to report.

References

1. Whetstone WD, Hsu JY, Eisenberg M, et al. Blood-spinal cord barrier after spinal cord injury: relation to revascularization and wound healing. *J Neurosci Res* 2003;74:227–239.
2. Tator CH, Fehlings MG. Review of the secondary injury theory of acute spinal cord trauma with emphasis on vascular mechanisms. *J Neurosurg* 1991;75:15–26.
3. Flanders AE, Schaefer DM, Doan HT, et al. Acute cervical spine trauma: correlation of MR imaging findings with degree of neurologic deficit. *Radiology* 1990;177:25–33.

4. Flanders AE, Spettell CM, Friedman DP, et al. The relationship between the functional abilities of patients with cervical spinal cord injury and the severity of damage revealed by MR imaging. *AJNR Am J Neuroradiol* 1999;20:926–934.
5. Flanders AE, Spettell CM, Tartaglino LM, et al. Forecasting motor recovery after cervical spinal cord injury: value of MR imaging. *Radiology* 1996;201:649–655.
6. Popovich PG, Longbrake EE. Can the immune system be harnessed to repair the CNS? *Nat Rev Neurosci* 2008;9:481–493.
7. Verkman AS. Mammalian aquaporins: diverse physiological roles and potential clinical significance. *Expert Rev Mol Med* 2008;10:e13.
8. Oshio K, Binder DK, Yang B, et al. Expression of aquaporin water channels in mouse spinal cord. *Neuroscience* 2004;127:685–693.
9. Nestic O, Lee J, Ye Z, et al. Acute and chronic changes in aquaporin 4 expression after spinal cord injury. *Neuroscience* 2006;143:779–792.
10. Vitellaro-Zuccarello L, Mazzetti S, Madaschi L, et al. Chronic erythropoietin-mediated effects on the expression of astrocyte markers in a rat model of contusive spinal cord injury. *Neuroscience* 2008;151:452–466.
11. Saadoun S, Bell BA, Verkman AS, Papadopoulos MC. Greatly improved neurological outcome after spinal cord compression injury in AQP4-deficient mice. *Brain* 2008;131:1087–1098.
12. Metz GA, Curt A, van de Meent H, et al. Validation of the weight-drop contusion model in rats: a comparative study of human spinal cord injury. *J Neurotrauma* 2000;17:1–17.
13. Young W. Spinal cord contusion models. *Prog Brain Res* 2002;137:231–255.
14. Ma T, Yang B, Gillespie A, et al. Generation and phenotype of a transgenic knockout mouse lacking the mercurial-insensitive water channel aquaporin-4. *J Clin Invest* 1997;100:957–962.
15. Basso DM, Fisher LC, Anderson AJ, et al. Basso Mouse Scale for locomotion detects differences in recovery after spinal cord injury in five common mouse strains. *J Neurotrauma* 2006;23:635–659.
16. Engesser-Cesar C, Anderson AJ, Basso DM, et al. Voluntary wheel running improves recovery from a moderate spinal cord injury. *J Neurotrauma* 2005;22:157–171.
17. Ma M, Basso DM, Walters P, et al. Behavioral and histological outcomes following graded spinal cord contusion injury in the C57Bl/6 mouse. *Exp Neurol* 2001;169:239–254.
18. Hoang TX, Pikov V, Havton LA. Functional reinnervation of the rat lower urinary tract after cauda equina injury and repair. *J Neurosci* 2006;26:8672–8679.
19. Inman D, Guth L, Steward O. Genetic influences on secondary degeneration and wound healing following spinal cord injury in various strains of mice. *J Comp Neurol* 2002;451:225–235.
20. Steward O, Schauwecker PE, Guth L, et al. Genetic approaches to neurotrauma research: opportunities and potential pitfalls of murine models. *Exp Neurol* 1999;157:19–42.
21. Manley GT, Fujimura M, Ma T, et al. Aquaporin-4 deletion in mice reduces brain edema after acute water intoxication and ischemic stroke. *Nat Med* 2000;6:159–163.
22. Bloch O, Papadopoulos MC, Manley GT, Verkman AS. Aquaporin-4 gene deletion in mice increases focal edema associated with staphylococcal brain abscess. *J Neurochem* 2005;95:254–262.
23. Papadopoulos MC, Manley GT, Krishna S, Verkman AS. Aquaporin-4 facilitates reabsorption of excess fluid in vasogenic brain edema. *FASEB J* 2004;18:1291–1293.
24. Maikos JT, Shreiber DI. Immediate damage to the blood-spinal cord barrier due to mechanical trauma. *J Neurotrauma* 2007;24:492–507.
25. Anderson TE, Stokes BT. Experimental models for spinal cord injury research: physical and physiological considerations. *J Neurotrauma* 1992;9(suppl 1):S135–S142.
26. Schwartz ED, Himes BT. New model of minimally invasive experimental spinal cord injury. *AJNR Am J Neuroradiol* 2003;24:166–168.
27. Ramos A, Ho WC, Forte S, et al. Hypo-osmolar stress induces p75NTR expression by activating Sp1-dependent transcription. *J Neurosci* 2007;27:1498–1506.
28. Hinson SR, Roemer SF, Lucchinetti CF, et al. Aquaporin-4-binding autoantibodies in patients with neuromyelitis optica impair glutamate transport by down-regulating EAAT2. *J Exp Med* 2008;205:2473–2481.
29. Zeng XN, Sun XL, Gao L, et al. Aquaporin-4 deficiency down-regulates glutamate uptake and GLT-1 expression in astrocytes. *Mol Cell Neurosci* 2007;34:34–39.
30. Park E, Velumian AA, Fehlings MG. The role of excitotoxicity in secondary mechanisms of spinal cord injury: a review with an emphasis on the implications for white matter degeneration. *J Neurotrauma* 2004;21:754–774.
31. Auguste KI, Jin S, Uchida K, et al. Greatly impaired migration of implanted aquaporin-4-deficient astroglial cells in mouse brain toward a site of injury. *FASEB J* 2007;21:108–116.
32. Herrmann JE, Imura T, Song B, et al. STAT3 is a critical regulator of astrogliosis and scar formation after spinal cord injury. *J Neurosci* 2008;28:7231–7243.
33. Okada S, Nakamura M, Katoh H, et al. Conditional ablation of Stat3 or Socs3 discloses a dual role for reactive astrocytes after spinal cord injury. *Nat Med* 2006;12:829–834.
34. Sroga JM, Jones TB, Kigerl KA, et al. Rats and mice exhibit distinct inflammatory reactions after spinal cord injury. *J Comp Neurol* 2003;462:223–240.
35. Bloch O, Auguste KI, Manley GT, Verkman AS. Accelerated progression of kaolin-induced hydrocephalus in aquaporin-4-deficient mice. *J Cereb Blood Flow Metab* 2006;26:1527–1537.
36. Seki T, Fehlings MG. Mechanistic insights into posttraumatic syringomyelia based on a novel in vivo animal model. Laboratory investigation. *J Neurosurg Spine* 2008;8:365–375.